Istraživanja i projektovanja za privredu
ISSN 1451-4117
DOI:10.5937/jaes0-42738
www.engineeringscience.rs

iipp publishing

Journal of Applied Engineering Science
Vol. 21, No. 3, 2023
Original Scientific Paper
Paper number: 21(2023)3, 1124, 827-836

INFLUENCES OF NONLINEAR SUSPENSION ON THE BUS'S ROLL STABILITY BY A LATERAL DYNAMIC 4-DOF MODEL

Huu Nhan Tran[1]*, Ngoc Dai Pham[1]

[1]Faculty of Transportation Engineering, Ho Chi Minh City University of Technology (HCMUT) – Vietnam National University Ho Chi Minh City, 268 Ly Thuong Kiet Street, District 10, Ho Chi Minh City, Vietnam
** thnhan@hcmut.edu.vn*

The influences of nonlinear suspension system with air spring and nonlinear asymmetrical (NA) absorber in comparison with a linear suspension is analyzed based on a lateral dynamic four degrees of freedom (4-DOF) model. The lateral dynamic model considers the effects of anti-roll bars, the roll center position, and the transient excitation of the road on the roll stability performance. The characteristics of the suspension system, the position of the roll center, the road excitation load all play very important roles in determining the roll stability of the vehicle. The maximum dynamic roll angle with nonlinear suspension is always smaller than that with linear suspension. The maximum dynamic rollover stability index is strongly dependent on the velocity and about 27% on average lower than that of linear suspension in the whole velocity domain, subjected under road excitation. However, the maximum of absolute acceleration is always larger with the nonlinear suspension system.

Keywords: rollover stability, roll center, lateral dynamic model, air spring, nonlinear asymmetric damper

1 INTRODUCTION

To meet the increasing demand for long-distance passenger transport, large size vehicles have been actively designed and manufactured by automobile manufacturing and assembly companies with a localization rate of over 50%. Therefore, conducting research to evaluate the dynamics directly related to the safety of vehicles is very necessary and consistent with the general development trend in the development strategy of the automobile industry in Vietnam. Especially, the research is to solve the problem of improving the design, increasing the safety during the operation of large size vehicles, contributing to reducing the number of traffic accidents. Moreover, traffic safety issues especially related to large size vehicles have been and are receiving a lot of attention in Vietnam.

The phenomenon of large size vehicles being rollover when an accident occurs during traffic participation shows the need to conduct research related to the roll stability [1,2]. Many studies have been carried out to solve the problem related to increasing the roll stability and safety. The roll angle, and the height of the vehicle's center of gravity from the roll center are two important parameters that directly affect the safety and roll stability of vehicles. The theoretical method of determining these two parameters in real time has been verified by experimental measurements with a low frequency tilt angle sensor and a gyroscope [3]. The roll angle and lateral acceleration together with inspection of lane departure obtained by a vehicle dynamic simulation model, which is a proposed technique to access the safety and accident prediction on expressways [3]. The influences of roll angle on roll stability with different suspension types and wheel camber angles has been studied [5]. The height of the center of gravity is used as a control parameter to predict the critical rollover stability condition, thereby controlling the brake force distribution system to increase the stability of the vehicle [3, 6]. Research on smartphone application in predicting vehicle rollover stability when turning or changing lanes, in which a new rollover speed prediction model is based on the derivation of three-degree-of-freedom vehicle dynamics and LTR, is presented [7]. The lateral load transfer rate is defined as the vehicle rollover evaluation index, which is used to control the speed of the electric motor to increase the roll stability of the electric vehicle [8]. Controlling the off-road vehicle suspension system reduces the roll angle to prevent rollover [9]. The roll angle control models in the lateral plane are employed to investigate the influences of the roll angle motion control on the roll stability features [10]. A study on rollover index and stability for a triaxle bus is carried out using a six degree of freedom rollover model of the triaxle bus, based on the LTR the rollover index established for the front and rear axles separately [11]. Therefore, it is necessary to conduct research to be able to evaluate the dynamic parameters affecting the roll stability and safety of large size vehicles. All contribute to determining the parameters as a design database to improve the safety and operation of these large size vehicles. The article derives a lateral dynamic model with 4-DOF, including the role of anti-roll bars, the influences of the roll center position, and the excitation effects from the road.

Calculations are carried out based on typical large size bus manufactured by Samco, Vietnam. The roll stability indexes are the roll angle and the LTR, which are determined and analyzed in the time domain, the excitation velocity domain from the road, and in the height of the center of gravity from the roll center domain. The obtained results are compared with both linear and nonlinear suspension systems to evaluate the vehicle's roll stability.

2 CALCULATION MODEL AND INPUT PARAMETERS

2.1 Lateral dynamic 4-DOF model

To study the lateral dynamic stability, the 4-DOF lateral dynamic model is employed, Fig. 1.

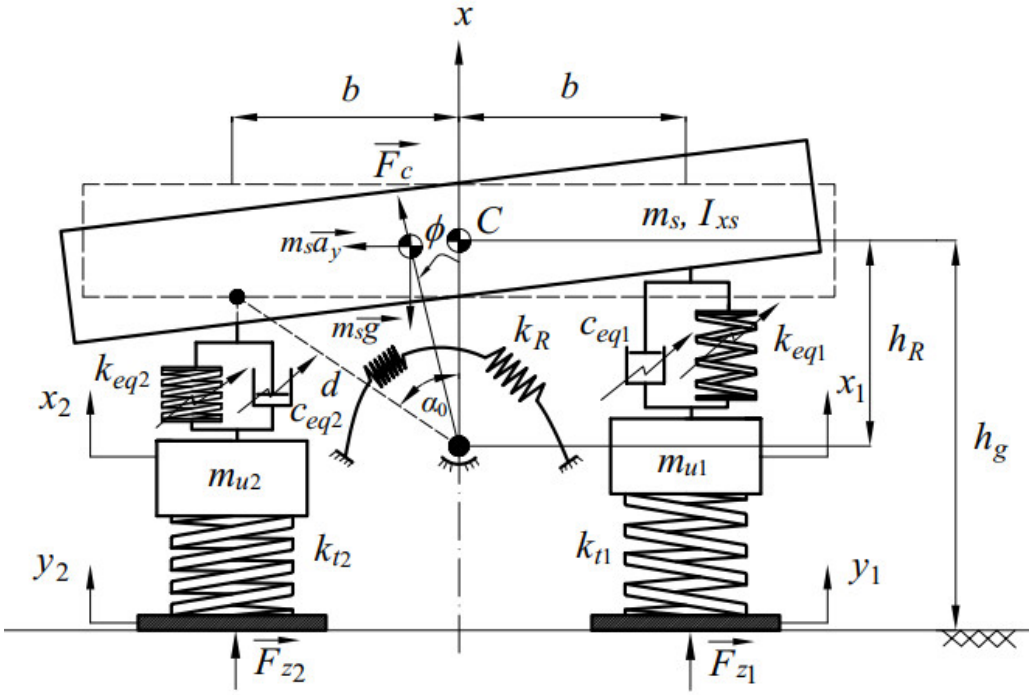

Fig. 1. The lateral dynamic 4-DOF model.

The model allows to investigate the lateral dynamic parameters of the vehicle body, or namely the sprung mass element in the vertical x direction, and its rotational motion about the position of the roll center. The under body components of the vehicle are modeled by two un-sprung masses on the left and right side, m_{u1} and m_{u2} respectively. The applied forces due to the lateral acceleration component a_y acting at the position of the vehicle's center of gravity, and due to the road excitation y_1, y_2 corresponding to the left and right side respectively.

The symbols, and the meanings of the lateral dynamic model parameters, are given in Table 1.

Table 1. The lateral dynamic 4-DOF model parameters

Symbol	Description	Value
m_s	Sprung mass [kg]	14,010
I_{xs}	Mass inertia moment of the bus body about the x axis [kg.m^2]	18,970
m_{u1}, m_{u2}	Un-sprung mass on the left and right side [kg]	1,940
k_{01}, k_{02}	Initial air spring stiffness on the left and right side [N/m]	339×10^3
c_{01}, c_{02}	Initial damping coefficient on the left and right side [Ns/m]	29,000
k_{t1}, k_{t2}	Tire stiffness on the left and right side [N/m]	2,400,000
k_R	Anti-roll bar stiffness [N/m]	112,376
x	Vertical displacement of the sprung mass [m]	-
x_1, x_2	Vertical displacement of the un-sprung mass on the left and right side [m]	-
ϕ	Roll angle of the sprung mass [rad]	-
y_1, y_2	Road excitation on the left and right side [m]	-
b	Distance from the center of gravity to the center of the left or right wheel [m]	0.98
h_g	The height of the sprung mass's center of gravity [m]	1.8
h_R	The height of the sprung mass's center of gravity from the roll center [m]	0.5÷1
α_0	The angle formed by two dimensional parameters of b and h_R [rad]	atan(b/h_R)

For simplicity, we consider the model to be symmetrical relative to the longitudinal plane of the vehicle, it means that the parameters of size, mass, suspension, tires, anti-roll, on the left and right sides are equal. The position of the roll center in the lateral plane lies on the axis *Ox* and is a distance h_R from the sprung mass's center of gravity *C*. The lateral plane in the model is formed by gradually narrowing the front and rear of the vehicle. Therefore, the parameters of mass, suspension, tires, anti-roll on the left and right sides of the vehicle are determined as the sum of the components of the front and rear parts corresponding to the left and right sides of the vehicle respectively.

The Doosan bus manufactured by Samco in Vietnam is investigated to determine the input parameters used for calculation.

The mechanical system is affected by the force components located at the vehicle's center of gravity, including: the lateral force component caused by the lateral acceleration a_y; The gravitational force when the gravity center deviate from the symmetrical position; And the centrifugal force component generated by the rotational motion of the vehicle body around the roll center, does not coincide with its center of gravity. In addition, the excitation effect from the uneven road surface y_1 and y_2 independently on the left and right sides of the vehicle, is also integrated in the model.

Differential equations describing vehicle lateral dynamic 4-DOF model, with a state variable vector $X = \begin{bmatrix} x & \phi & x_1 & x_2 \end{bmatrix}^{'}$ is written in the general matrix form, as shown in equation (1).

$$[m]\ddot{X} + [c]\dot{X} + [k]X = [F] \tag{1}$$

Where, the mass matrix [*m*], stiffness matrix [*k*] with instantaneous stiffness of the nonlinear air-springs determined according to the displacement value and its state of extension or compression, presented in detail in the section 2.2 below. Similarly, damping coefficient matrix [*c*] with instantaneous damping coefficient of asymmetrical nonlinear absorbers determined according to the value of motion velocity and its state of extension or compression, presented in detail in the section 2.3. The vector of the applied force components [*F*] and the matrices included in the general dynamic equation (1), are presented below.

$$X = \begin{bmatrix} x \\ \phi \\ x_1 \\ x_2 \end{bmatrix}; \quad \dot{X} = \begin{bmatrix} \dot{x} \\ \dot{\phi} \\ \dot{x}_1 \\ \dot{x}_2 \end{bmatrix}; \quad \ddot{X} = \begin{bmatrix} \ddot{x} \\ \ddot{\phi} \\ \ddot{x}_1 \\ \ddot{x}_2 \end{bmatrix}$$

$$[m] = \begin{bmatrix} m_s & 0 & 0 & 0 \\ 0 & I_{xs} + m_s h_R^2 & 0 & 0 \\ 0 & 0 & m_{u1} & 0 \\ 0 & 0 & 0 & m_{u2} \end{bmatrix}$$

$$[k] = \begin{bmatrix} k_{eq1} + k_{eq2} & d\sin\alpha_0\left(k_{eq1} - k_{eq2}\right) & -k_{eq1} & -k_{eq2} \\ d\sin\alpha_0\left(k_{eq1} - k_{eq2}\right) & d^2\sin^2\alpha_0\left(k_{eq1} + k_{eq2}\right) + k_R & k_{eq1}d\sin\alpha_0 & -k_{eq2}d\sin\alpha_0 \\ -k_{eq1} & k_{eq1}d\sin\alpha_0 & k_{eq1} + k_{t1} & 0 \\ -k_{eq2} & -k_{eq2}d\sin\alpha_0 & 0 & k_{eq2} + k_t \end{bmatrix}$$

$$[c] = \begin{bmatrix} c_{eq1} + c_{eq2} & -d\sin\alpha_0\left(c_{eq1} - c_{eq2}\right) & -c_{eq1} & -c_{eq2} \\ -d\sin\alpha_0\left(c_{eq1} - c_{eq2}\right) & d^2\sin^2\alpha_0\left(c_{eq1} + c_{eq2}\right) & c_{eq1}d\sin\alpha_0 & -c_{eq2}d\sin\alpha_0 \\ -c_{eq1} & c_{eq1}d\sin\alpha_0 & c_{eq1} & 0 \\ -c_{eq2} & -c_{eq2}d\sin\alpha_0 & 0 & c_{eq2} \end{bmatrix}$$

$$[F] = \begin{bmatrix} k_{eq1}h_R - k_{eq2}h_R - k_{eq1}d\cos\alpha_0 + k_{eq2}d\cos\alpha_0 + F_c\cos\phi \\ M_{x\_ay} + M_{x\_g} + F_c\sin\phi\left(h_R\cos\phi + x\right) - F_c\cos\phi h_R\sin\phi - k_{eq1}h_R d\sin\alpha_0 + \\ -k_{eq2}h_R d\sin\alpha_0 + k_{eq1}d^2\sin\alpha_0\cos\alpha_0 + k_{eq2}d^2\sin\alpha_0\cos\alpha_0 \\ k_{t1}y_1 - k_{eq1}h_R + k_{eq1}d\cos\alpha_0 \\ k_{t2}y_2 + k_{eq2}h_R + k_{eq2}d\cos\alpha_0 \end{bmatrix}$$

2.2 Air-spring

The suspension system includes an air-spring element. Based on the variable parameter between displacement and the force at the pressure value of the air-spring used on the vehicle, the corresponding stiffness of the air-spring is determined, k_{eq}. The 3rd order polynomial interpolation method is employed to calculate air-spring stiffness based on the instantaneous displacement value relative to the initial equilibrium position of the air-spring corresponding to the extension or compression stroke. The initial leveling position of the air-spring is assumed to be mean value of the displacement of the air-spring relative to the applied force. The observed bus is designed with one air-spring in the front and two in the rear, the stiffness of the air-spring on each left or right side of the bus is the sum of the stiffness of all three front and rear air-springs totally. The experimental and interpolated stiffness variation curves, the 3rd order polynomial used to calculate the front suspension relative to the displacement around the equilibrium position are shown in Fig. 3. The stiffness at the initial equilibrium, k_0=339×10^3 is equivalent to a natural frequency close to 1 (Hz), which is the usual natural frequency of common vehicle suspension systems, [12].

The range of working stroke of the air-spring is ±0.125 (m).

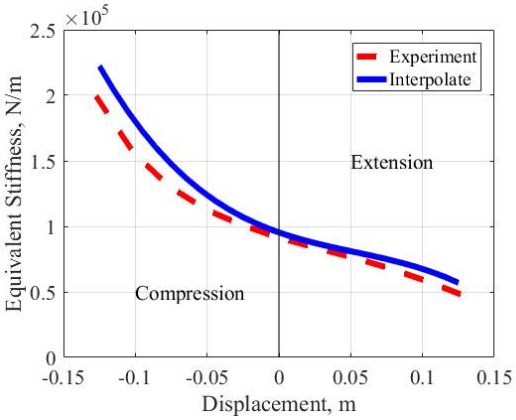

Fig. 2. Equivalent stiffness versus displacement of the front air-spring, experimental and polynomial interpolation.

2.3 Asymmetric nonlinear absorber

The initial damping coefficient is chosen so that c_0=29,000 (Ns/m) to perform the calculation, corresponding to the damping ratio value ξ=0.3, as in (2), [12].

$$\xi = \frac{c_0}{2\sqrt{m_{s1}k_{s1}}} \tag{2}$$

Where m_{s1} and k_{s1} are the mass of the sprung mass and the total stiffness of the three air-springs on the left side of the vehicle, respectively. With the initial condition, the damping coefficient is equivalent to c_{eq}=c_0, when the damping force is equivalent to zero, F_{eqD}=0. When the system is subjected to an external applied force, F_{eqD}≠0, the equivalent damping coefficient, c_{eq} is determined based on parameters including: the equivalent damping force F_{eqD}, suspension relative velocity, and whether the stroke is extended or compressed. The selected asymmetry coefficient corresponding to the 30/70 asymmetry ratio is e_D=0.4, it is a common symmetric coefficient [13]. The equivalent damping coefficient changes when the velocity dx reaches the knee-point critical value dx_c=0.05 (m/s), with coefficients κ=1, λ=2.

Equivalent damping force value is calculated according to (3).

$$F_{eqD} = \begin{cases} \kappa c_0 \mathrm{d}x(1-e_D); \\ \quad \text{if } \mathrm{d}x<0, \text{and} \left|\mathrm{d}x\right| \le \mathrm{d}x_c \\ (1-e_D)c_0\left[\lambda \mathrm{d}x-(\kappa-\lambda)\mathrm{d}x_c\right]; \\ \quad \text{if } \mathrm{d}x<0, \text{and} \left|\mathrm{d}x\right| > \mathrm{d}x_c \\ \kappa c_0 \mathrm{d}x(1+e_D); \\ \quad \text{if } \mathrm{d}x>0, \text{and} \, \mathrm{d}x \le \mathrm{d}x_c \\ (1+e_D)c_0\left[\lambda \mathrm{d}x+(\kappa-\lambda)\mathrm{d}x_c\right]; \\ \quad \text{if } \mathrm{d}x>0, \text{and} \, \mathrm{d}x > \mathrm{d}x_c \end{cases} \tag{3}$$

The variation characteristics of the equivalent damping force, F_{eqD} relative to the velocity dx, for the case of linear damping coefficient c_0, and nonlinear one with the equivalent damping coefficient c_{eq}, are shown in Fig. 3.

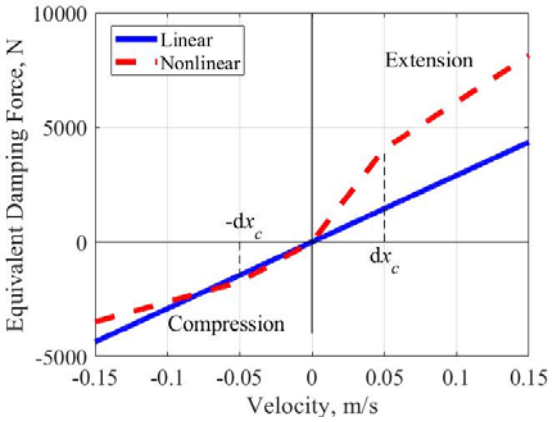

Fig. 3. Variation characteristics of the equivalent damping force versus velocity

2.4 The external applied loadings

To be able to capture the most dangerous scenarios that can realistically occur. Then, the step function is assumed to be able to fully capture all abrupt changes of the vehicle's lateral acceleration. It is employed to describe the variation of the lateral acceleration component in the time domain to perform the calculation to determine the lateral dynamic parameters of the vehicle body. The initial value of zero, and the selected stability value is the maximum value ($a_{y,\text{lift-off}}$) to ensure safety according to the vehicle's rollover conditions, (4), [10], in which the maximum value of inclination angle is selected, $\phi_{\max} = 10^0$.

$$a_{y,\text{lift-off}} = \frac{b - h_R \phi_{\max}}{h_g} \tag{4}$$

The applied moment due to the lateral acceleration a_y is determined according to (5).

$$M_{x\_ay} = m_s a_y (h_R \cos\phi + x) \tag{5}$$

The applied moment due to the force of gravity is determined according to (6).

$$M_{x\_g} = m_s g h_R \sin\phi \tag{6}$$

The centrifugal force at the position of gravity center caused by the roll motion of the sprung mass around the roll center is determined according to (7).

$$F_c = m_s (h_R + x\cos\phi)\dot{\phi}^2 \tag{7}$$

The centrifugal force is directed on the coordinate system into 2 components that cause translational and rotational motion of the sprung mass.

2.5 Road profile

To perform the calculation of the lateral dynamics of the vehicle body in the case of road excitation when moving with a velocity value v, we use a semi-squared sinusoidal function, (8), [14]:

$$y = \begin{cases} d_2 \sin^2 \dfrac{\pi v}{d_1} t; & 0 \le t < \dfrac{d_1}{v} \\ 0; & t < 0,\ t \ge \dfrac{d_1}{v} \end{cases} \tag{8}$$

With the length d_1 = 3.7 (m); And the bump height d_2 = 0.1 (m).

3 RESULTS AND DISCUSSION

Calculations are carried out with linear suspension, with constant spring stiffness and damping coefficient throughout the calculation. These values are chosen to be the initial values at the equilibrium position of the system. Similar calculations are made with nonlinear suspension, spring stiffness and damping coefficient vary during the calculation according to the relative displacement, velocity of the suspension, and the state of suspension's stroke, as presented in sections 2.2 and 2.3, respectively.

Calculations are carried out for different specific cases to determine and compare the dynamic rollover stability parameters of the sprung mass with linear and nonlinear suspension.

3.1 In the time domain

To investigate the roll angle in the time domain, for 2 cases of linear and nonlinear suspension systems, calculations are carried out with h_R=0.5 (m), without road excitation. The roll angle versus time for the case of linear and nonlinear suspension is shown in Fig. 4. Due to the stiffer nonlinear suspension, with a larger damping coefficient at low

velocity, the air spring is stiffer in compression. Therefore, the maximum roll angle is smaller and more stable than in the case of a linear suspension.

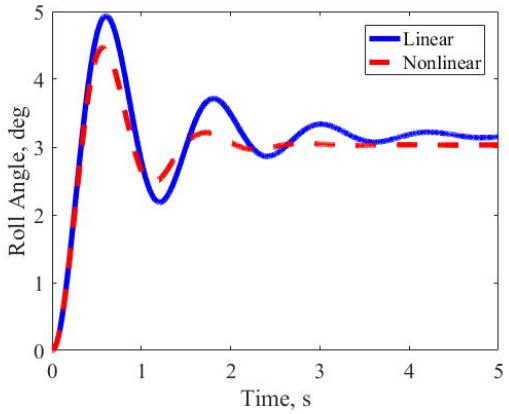

Fig. 4. Roll angle in the time domain

To investigate the effect of the road excitation on the variation of the roll angle and the acceleration of the sprung mass, $\ddot{x}_s$ in the time domain, the calculation is performed similarly to above, however, with the consideration of the effect of road excitation on the right side of the model only (y_1), as in Fig. 1, with speed of v=40 (km/h). In the case of nonlinear suspension, the roll angle in the time domain with and without road excitation effect is shown in Fig. 5. The roll angle value reaches the maximum and reaches the stable value at the same time with and without the road excitation effect. However, the maximum value obtained in the case of road excitation effects increases by more than 16%. Thus, the road excitation significantly increases the maximum value of the roll angle and does not affect its value at steady state.

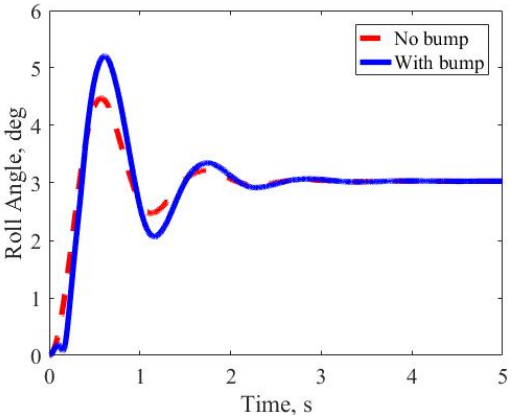

Fig. 5. Roll angle in the time domain, in case of nonlinear suspension

The sprung mass acceleration ratio $\ddot{x}_s/g$, where g is the gravity acceleration, in the time domain with linear and nonlinear suspensions is shown in Fig. 6. The obtained results show that, the maximum absolute acceleration ratio for the nonlinear suspension case increased by 24% compared with the linear case, the more rigid the suspension, the greater the acceleration [12].

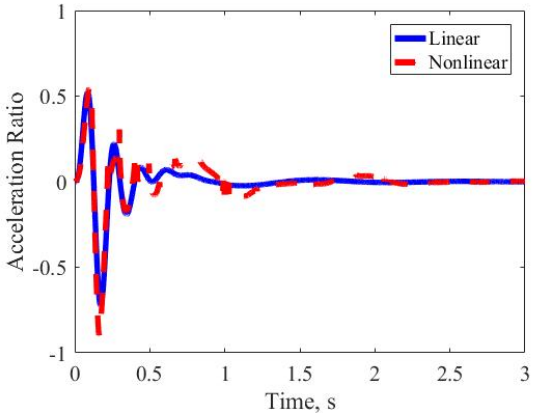

Fig. 6. Acceleration ratio in the time domain

3.2 In the velocity domain with road excitation

With consideration of both the linear and nonlinear cases, under the road excitation effect with the above parameters, the range of velocity from 20÷120 (km/h), h_R=0.5 (m). With each value of velocity, we can determine the lateral dynamic parameters in the time domain as in section 3.1, and respectively we can determine the maximum value, and the steady-state value.

The maximum roll angles, and steady-state ones in the velocity domain with two types of suspension are shown in Fig. 7.

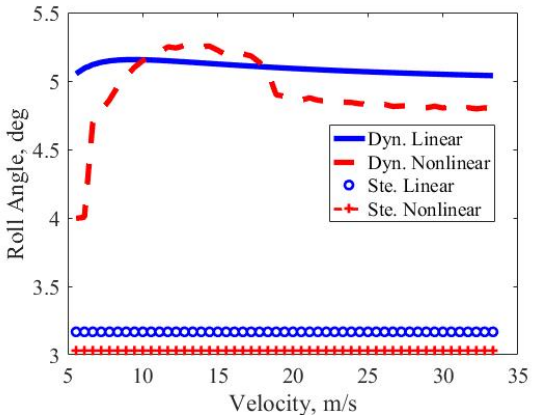

Fig. 7. Roll angle in the velocity domain

The mean value of maximum dynamic roll angles is always greater than the steady-state one by about 60% in the whole observed velocity domain with both linear and nonlinear suspension systems. In the low velocity value region v<10 (m/s), the maximum dynamic roll angle with nonlinear suspension is much smaller than in the linear case, because at low velocity the nonlinear damping coefficient is larger or stiffer nonlinear suspension. In the region of higher velocity, the maximum dynamic roll angle is always a bit higher than in the nonlinear case, corresponding to the velocity range of v=10÷20 (m/s) and decreases slightly when v>20 (m/s), Fig. 7. The steady-state roll angle value with linear suspension is very little higher than that of nonlinear suspension and is almost constant throughout the velocity domain. In the case of a linear suspension system, the maximum value of the dynamic roll angle changes only slightly at the velocity range corresponding to the rapid increasing and creating a large difference as with nonlinear suspension, and almost unchanged in the velocity domain. However, the maximum difference of the maximum dynamic roll angle is only close to 5% between the linear and nonlinear suspension in the velocity domain, or the maximum dynamic roll angle does not depend much on the velocity in the case of road excitation.

The obtained ratio of maximum absolute acceleration, $\max\left|\ddot{x}_s\right|/g$ at each velocity value varies over the velocity domain, as shown in Fig. 8.

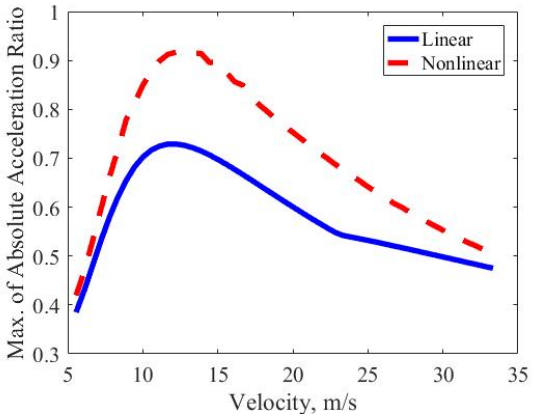

Fig. 8. Maximum absolute acceleration ratio in the velocity domain

The ratio of maximum absolute acceleration is always greater with stiffer nonlinear suspension than with softer linear suspension, throughout the velocity domain. The difference reaches the maximum value of about 26% in the velocity domain v=10÷20 (m/s), corresponding to the dynamic roll angle in the velocity domain with the largest difference as shown in Fig. 7. The maximum acceleration is significantly increased under the road excitation. And it is also significantly dependent on the velocity.

Rolling motion causes a change in the vertical reaction force distribution at the wheels on the left F_{z2} and the right F_{z1}, namely the load transfer ratio (LTR), which is defined as an index to evaluate the rollover stability of the vehicle, according to (9), the vehicle reaches the critical rollover stability when the LTR reaches a value of 1, [3].

$$LTR = \frac{F_{z2} - F_{z1}}{F_{z2} + F_{z1}} \tag{9}$$

Where, the vertical reaction force at the wheel on each side is determined with respect to time at each value of velocity, (10).

$$F_{z1} = k_{t1}x_1 + \frac{mg}{2}; \qquad F_{z2} = k_{t2}x_2 + \frac{mg}{2} \tag{10}$$

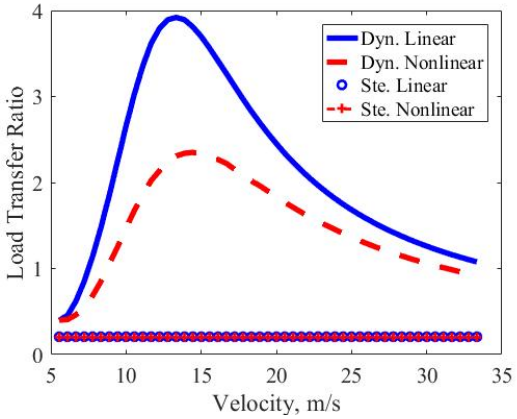

Fig. 9. LTR in the velocity domain

The maximum dynamic rollover stability index (LTR_{dyn}) and the steady-state one (LTR_{ste}) in the velocity domain are shown in Figure 9. The obtained results show that for the case of nonlinear suspension system, LTR_{dyn} is always with an average of about 27% lower than that of linear suspension in the whole velocity domain. Especially, the peak value of LTR_{dyn} with nonlinear suspension is about 40% lower than that of linear suspension. In addition, the steady-state rollover stability index, LTR_{ste} remains constant and is almost equal in the velocity domain with both types of suspension. The value of LTR_{dyn} is 3÷4 times larger than the LTR_{ste} corresponding to the linear suspension, and it is about 1÷2 times larger with the nonlinear suspension. Therefore, the velocity has almost no effect on the variation of LTR_{ste}, whereas it causes a significant increase in the LTR_{dyn}. Although the obtained LTR_{dyn} shows that roll stability is not guaranteed under the above applied loadings, the LTR_{dyn} of the bus with nonlinear suspension has significantly improved roll stability on average about 27% in the whole observed velocity domain.

3.3 In the h_R domain

The height of the sprung mass's center of gravity from the roll center of the sprung mass, h_R is chosen to be in the range from 0.5÷1 (m) for investigation. Similarly, the calculation process is carried out in the same way as above, but without considering the road excitation, for both suspension cases.

The maximum dynamic roll angle and steady state roll angle in the h_R domain for both suspension cases are shown in Fig. 10. The roll angle increases linearly with roughly equal slope in the h_R domain, the maximum dynamic roll angle and the steady-state roll angle are always slightly larger than in the case of the linear suspension. The difference of the maximum dynamic roll angles between the two suspension cases is larger than that of the steady state roll angles. The mean of maximum dynamic roll angle is 50÷60% larger than the mean of steady-state roll angle in the h_R domain for both suspension cases. The maximum dynamic roll angle increased by 100% corresponds to the h_R increase of 100% in the range of observation.

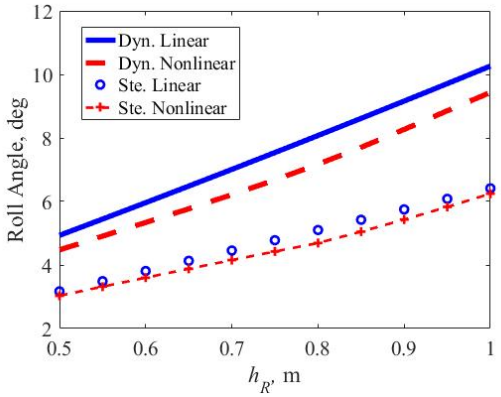

Fig. 10. Roll angle in the h_R domain

The maximum dynamic rollover stability index, LTR_{dyn} and at steady-state, LTR_{ste} in the h_R domain are presented in Fig. 11.

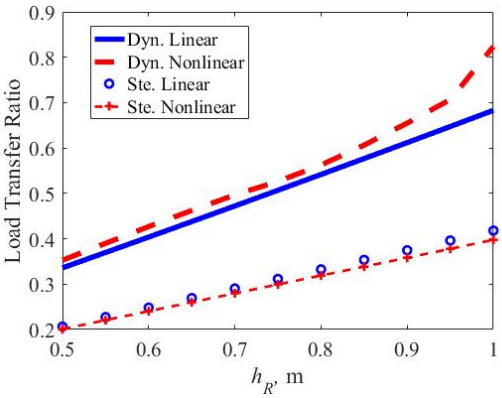

Fig. 11. LTR in the h_R domain

Similar to the variation of roll angle in the h_R domain, LTR_{dyn} and LTR_{ste} also increased linearly in the h_R domain for both suspension cases, Fig. 11. The mean of LTR_{dyn} with the case of nonlinear suspension is always about 7% larger than the case of linear suspension, in the observed domain of h_R. The mean of LTR_{dyn} is always about 81% and 62% larger than the mean of LTR_{ste} for the case of nonlinear and linear suspensions in the whole range of observation domain of h_R, respectively. For the two suspension types, the roll stability indexes at steady state LTR_{ste} are almost equal and increase proportionally to h_R with a smaller slope than that of the LTR_{dyn}. The slope of the LTR_{dyn} with the nonlinear suspension is the largest. Specifically, an increase of about 100% in LTR_{dyn} corresponds to a 100% increase in h_R in the range of observation.

4 CONCLUSIONS

The roll angle and the rollover stability indexes play a very important role in the evaluation of the vehicle's rollover stability. The obtained results are analyzed with 2 cases of linear and nonlinear types of suspension. Calculations are carried out with the lateral acceleration in the form of a step function, the range of h_R, and the road excitation with the range of velocity.

The obtained results are analyzed in the time domain, the h_R domain, and the velocity domain with the consideration of road excitation.

The obtained roll angle with the linear suspension system is always larger than that with the nonlinear suspension system. Especially, when subjected to the road excitation at low speed, the maximum dynamic roll angle is smaller significantly with the nonlinear suspension. However, in contrast to the maximum of absolute acceleration is always larger with the nonlinear suspension.

The effect of road excitation increases the maximum dynamic roll angle compared to the steady-state roll angle by about 60% on average. The maximum of absolute acceleration ratio with nonlinear suspension is always larger and depends heavily on the velocity in case of road excitation. For the case of nonlinear suspension system, the maximum dynamic rollover stability index, LTR_{dyn} is always with an average of about 27% lower than that of linear suspension in the whole velocity domain, and it is significantly dependent on velocity.

Whereas, in the h_R domain, the sudden change in the form of a step function of the applied load significantly increases the value of the maximum dynamic roll angle and rollover stability index, compared with the roll angle and the rollover stability index in steady state, respectively. The maximum dynamic roll angle, and the maximum dynamic rollover stability index increase by about 100%, corresponding to the 100% increase of h_R in the range of observation.

5 ACKNOWLEDGEMENTS

We acknowledge Ho Chi Minh City University of Technology (HCMUT), VNU-HCM for supporting this study.

6 REFERENCES

[1] Socialist Republic of Vietnam - Ministry of Transport, from *https://mt.gov.vn/vn/tin-tuc-bvcd/1020/34383/dan-thich-nhung-di-xe-khach-giuong-nam-co-an-toan.aspx*, accessed on 2022-02-07.

[2] Nurzaki Ikhsan, Ahmad Saifizul, Rahizar Ramli, (2021). The effect of vehicle and road conditions on rollover of commercial heavy vehicles during cornering: a simulation approach. *Sustainability*, vol 13, issue 11, 6337, DOI: https://doi.org/10.3390/su13116337.

[3] Rajamani, R., (2009). Real-Time Estimation of Roll Angle and CG Height for Active Rollover Prevention Applications. American Control Conference, p. 433-438.

[4] Eko Deprianto, Ming Foong Soong, Rahizar Ramli, Ahmad Abdullah Saifizul, (2020). Safety assessment and accident prediction on expressways using vehicle dynamic simulation technique. *International Journal of Scientific & Technology Research*, vol 9, issue 1, 1856-1866.

[5] Parczewski, K., Wnęk, H., (2017). The influence of vehicle body roll angle on the motion stability and maneuverability of the vehicle*. Combustion Engines*, vol 168, no. 1, 133-139, DOI: 10.19206/CE-2017-121.

[6] Momiyama, F., Kitazawa, K., Miyazaki, K., Soma, H., Takahashi, T., (1999). Gravity center height estimation for the rollover compensation system of commercial vehicles. *JSAE Review 20*, p. 493-497.

[7] Chu, D., Li, Z., Wang, J., Wu, C., Hu, Z., (2018). Rollover speed prediction on curves for heavy vehicles using mobile smartphone. *Measurement*, vol 130, 404–411, DOI: 10.1016/j.measurement.2018.07.054.

[8] Jiang, F., Dong, M., Fan, Y., Wang, Q., (2022). Research on Motor Speed Control Method Based on the Prevention of Vehicle Rollover. *Energies*, vol 15, no. 10, 3609, DOI: 10.3390/en15103609.

[9] Van Der Westhuizen, S. F., Els, P. S., (2013). Slow active suspension control for rollover prevention. *Journal of Terramechanics*, vol 50, no. 1, 29–36, DOI: 10.1016/j.jterra.2012.10.001.

[10] Chokor, A., Talj, R., Doumiati, M., Charara, A., (2020). Effect of Roll Motion Control on Vehicle Lateral Stability and Rollover Avoidance. American Control Conference (ACC 2020), p. 4868-4875.

[11] Jin, Z., (2019). Study on Rollover Index and Stability for a Triaxle Bus. *Chinese Journal of Mechanical Engineering*, vol 32, no. 1, 32-64, DOI: 10.1186/s10033-019-0376-0.

[12] Gillespie D., (1992). *Fundamentals of Vehicle Dynamics*. SEA, USA.

[13] Dixon, J. C., (2007). *The Shock Absorber Handbook*. John Wiley & Sons, Ltd, USA, p 259-265.

[14] The Indian Roads Congress, IRC-99-1988, Tentative Guidelines on the Provision of Speed Breakers for Control of Vehicular Speeds on Minor Roads.

Paper submitted: 08.02.2023.

Paper accepted: 01.06.2023.